

The External Magnetic Field Created by the Superposition of Identical Parallel Finite Solenoids

Melody Xuan Lim* and Henry Greenside†

Department of Physics, Duke University, Durham NC 27708-0305

(Dated: July 31, 2015)

Abstract

Using superposition and numerical approximations of an analytical expression for the magnetic field generated by a finite solenoid, we show that the magnetic field external to parallel identical solenoids can be nearly uniform and substantial, even when the solenoids have lengths that are large compared to their radii. We study two arrangements of solenoids—a ring of parallel solenoids whose surfaces are tangent to a common cylindrical surface and to nearest neighbours, and a large finite hexagonal array of parallel solenoids—and summarize how the magnitude and uniformity of the resultant external field depend on the solenoid length and distances between solenoids. We also report some novel results about single solenoids, e.g., that the energy stored in the internal magnetic field exceeds the energy stored in the spatially infinite external magnetic field for even short solenoids. These results should be broadly interesting to undergraduates learning about electricity and magnetism as novel examples of superposition based on a familiar source of magnetic fields.

I. INTRODUCTION

In introductory physics courses on electricity and magnetism¹ and in upper-level undergraduate courses on electrodynamics^{2,3}, students learn a striking fact which is that the magnetic field \mathbf{B} generated by a sufficiently long cylindrical solenoid is highly uniform inside and of small magnitude outside. An implication of this fact is that the external magnetic field generated by a solenoid can usually be ignored as small.

But this well-known result raises some questions that are often not discussed in undergraduate courses. One question is how long must a solenoid actually be for the external magnetic field to be smaller than some specified value, at different points in space? And might there be circumstances in which the external magnetic field of several solenoids could combine to become substantial in magnitude, even for long solenoids? If so, might there also be configurations of solenoids such that their external magnetic field is also approximately uniform, so that a single solenoid or a pair of Helmholtz coils² is not the only way to generate an approximately uniform magnetic field in some region of space?

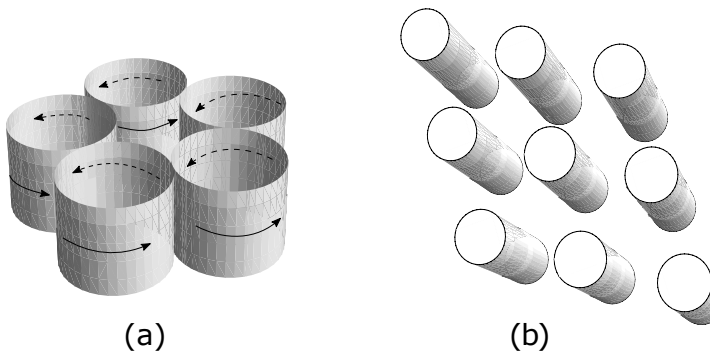


FIG. 1: Perspective drawings of two geometric arrangements of parallel identical solenoids.

- a) A ring of 5 solenoids, each of which is tangent to nearest neighbors and to a common inner cylindrical surface. The direction of the constant current density ι on the surface of the solenoids is indicated by the arrows. b) A section of an extended hexagonal array of parallel solenoids.

In this paper, we investigate these questions for two geometric arrangements of identical parallel solenoids (see Fig. 1), a ring of solenoids each of which is tangent to nearest neighbors and to a common inner cylindrical surface, and an extended hexagonal array. For both

cases, we find that there is a range of parameters (spacing of the solenoids and length of the solenoids for a given current density) for which the external magnetic field is substantial in magnitude, i.e., comparable to the magnitude of the field at the center of a long solenoid. Further, for a large hexagonal array of solenoids, the magnetic field between the solenoids is highly uniform and decreases slowly in magnitude with increasing solenoid length.

As part of our analysis, we also discuss some calculations and insights regarding the magnetic field of a single finite solenoid. For example, we calculate how the external magnetic field of a single solenoid decreases with increasing solenoid length for points ranging between close to and far from the solenoid's surface and find that a simple analytical expression derived for the far-field of a solenoid on its symmetry plane (see Eq. (6) below) gives a surprisingly accurate approximation of the magnetic field even close to the surface of the solenoid, at least for solenoids whose lengths exceed about four radii. This result unifies several previous discussions. We also show that the energy associated with the internal magnetic field of a solenoid exceeds the energy associated with the infinitely extended external magnetic field once the solenoid length exceeds about the radius of the solenoid, so comparing the internal and external magnetic energies does not lead to a new length scale that could be used to distinguish long from short solenoids (see Fig. 5 below).

While most of our results are new, parts of our Section II overlap with some previous papers. Brown and Flax⁴ discuss a way to calculate the magnetic field of a thick solenoid starting from the same integrals we use¹¹ for a zero-thickness solenoid, and Derby and Olbert⁷ has a closely related discussion that discusses a simple code to approximate these integrals using elliptic functions. Farley and Price⁵ show that the magnetic field strength just outside and on the midplane of a long finite solenoid of arbitrary constant cross-section falls off as L^{-2} with increasing L but these authors do not discuss, as we do for solenoids of circular cross section, how the magnetic field behaves for short solenoids or for points that are at intermediate distances from the solenoid's surface. Muniz et al.⁶ used Taylor expansions of the magnetic scalar potential to calculate the off-axis internal magnetic field of a finite solenoid, which complements our direct approximation of two one-dimensional integrals using numerical integration, although our method works for any point in space. However, these earlier papers do not mention some of our single solenoid results such as how the external magnetic energy compares with the internal magnetic energy, or how there is a simple expression that provides an accurate approximation of the magnetic field on the

midplane of a solenoid, for all points, not just close to the solenoid's surface. We also do not know of previous discussions about the magnetic field created by multiple parallel solenoids, which is the key contribution of this paper.

Our results should be of broad interest to undergraduate physics students and to instructors of undergraduate physics courses as a moderately more complicated example of superposition of magnetic fields, based on an example—a finite solenoid—that students have already learned about. The example we discuss below for a ring of parallel solenoids shows that just having a high symmetry of sources (many identical solenoids tangent to an inner cylinder) is not enough to guarantee uniformity of the external magnetic field. The second example of a large hexagonal array of parallel solenoids also shows that the external magnetic field of solenoids can be substantial, even for solenoids whose lengths are large compared to their radii. Finally, this paper provides a useful example to share with students of how software like Mathematica⁸, Maple⁹, and Matlab¹⁰ makes it easy for undergraduates to study numerically and visually superpositions of magnetic sources that are complicated by their number or geometry.

The rest of this paper is organized as follows. In the next section, we discuss a previously published analytical result^{7,11} for the magnetic field generated by an idealized cylindrical continuous solenoid and some insights about this field based on numerical studies of the analytical solution. In Section III, we use the results of Section II to discuss the properties of the magnetic field generated by a ring of identical parallel continuous solenoids, while in Section IV we discuss the properties of the magnetic field generated by a large hexagonal grid of identical parallel continuous solenoids. After summarizing key points in Section V, we discuss in Appendix A how various numerical calculations were validated, and in Appendix B how the radial components of the magnetic fields from different solenoids were combined.

II. THE MAGNETIC FIELD OF A SINGLE FINITE CONTINUOUS SOLENOID

The starting point for our study of the external magnetic field created by superimposing the fields of several parallel finite solenoids is an analytical expression^{7,11}, detailed below, for the magnetic field \mathbf{B} generated by a continuous solenoid, by which we mean a cylindrical surface of radius a and length L such that a spatially uniform time-independent one-dimensional current density ι (with units of amperes per meter) flows azimuthally around

the surface.

In this section, we discuss some physical properties of this analytical expression, for example we characterize how the external magnetic field depends on its length L , and confirm and extend an analytical result below that the external magnetic field at some point in space first increases and then decreases with increasing L , with an asymptotic function behavior of L^{-2} . We also compare the energy associated with the external magnetic field with the energy associated with the internal magnetic field as a function of L/a and find that the two energies become comparable when $L \approx a$, so that there is not an interesting new length scale for solenoids related to the magnetic energy.

A continuous solenoid is an idealization of real solenoids that are helically wound with wires of some finite thickness. The continuous solenoid has the advantage over real solenoids of requiring just three parameters to specify—a radius a , length L , and uniform current density ι —and has the further advantage that the analytical expression for its magnetic field is easy to evaluate numerically, accurately and quickly, at any point in space. The continuous solenoid is somewhat unphysical in that the zero-thickness of the surface causes the radial component of the magnetic field to diverge in magnitude at the top and bottom edges of the solenoid’s surface (see Fig. 3(a)), while no such divergence occurs for physical solenoids of finite thickness. However, we show below in this section that this divergence is not important since it still leads to a finite amount of energy stored in the magnetic field, and that the region where B_r has a large magnitude has a small spatial extent (compared to the solenoid’s radius) so that the magnetic field of the continuous solenoid provides quantitatively useful insights about the magnetic field of physical solenoids.

To describe the axisymmetric magnetic field of a continuous solenoid of radius a , length L , and current density ι , we introduce a cylindrical coordinate system (r, θ, z) such that $r = 0$ defines the solenoid’s axis and the plane $z = 0$ bisects the solenoid (so the ends of the solenoid lie at the coordinates $z = \pm L/2$). For this coordinate system, the current density ι flows counter-clockwise, so that the solenoid’s internal magnetic field \mathbf{B} points in the positive $\hat{\mathbf{z}}$ direction. From the azimuthal symmetry of the problem, we deduce that $B_\theta = 0$, and furthermore that B_z and B_r do not depend on θ , so that the magnetic field has the form

$$\mathbf{B} = B_r(r, z)\hat{\mathbf{r}} + B_z(r, z)\hat{\mathbf{z}}. \tag{1}$$

Calculations then show^{7,11} that the magnetic field at a point (r, z) in space has components

given in terms of the following one-dimensional integrals:

$$B_r = -\frac{a\mu_0\iota}{2\pi} \int_0^\pi d\alpha \left[\frac{\cos \alpha}{\sqrt{\xi^2 + r^2 + a^2 - 2ar \cos \alpha}} \right]_{\xi_-}^{\xi_+}, \quad (2)$$

$$B_z = \frac{a\mu_0\iota}{2\pi} \int_0^\pi d\alpha \left[\frac{\xi (a - r \cos \alpha)}{(r^2 + a^2 - 2ar \cos \alpha) \sqrt{\xi^2 + r^2 + a^2 - 2ar \cos \alpha}} \right]_{\xi_-}^{\xi_+}. \quad (3)$$

The lengths ξ_\pm are defined by

$$\xi_\pm = z \pm \frac{L}{2}, \quad (4)$$

and the notation $[f(\xi)]_{\xi_-}^{\xi_+}$ is an abbreviated way of writing $f(\xi_+) - f(\xi_-)$.

Appendix A gives details of how we approximated Eqs. (2) and (3) numerically for given values of r , z , a , L , and ι using Mathematica⁸. This appendix also summarizes how we validated the numerical approximations of these integrals, and results obtained for superpositions of solenoids. We found that Mathematica's numerical approximations to Eqs. (2) and (3) had a relative accuracy that exceeded eight significant digits, except for the component B_r near the coordinates $(r, z) = (a, \pm L/2)$, where this component diverges to infinity. This accuracy was more than adequate for our calculations.

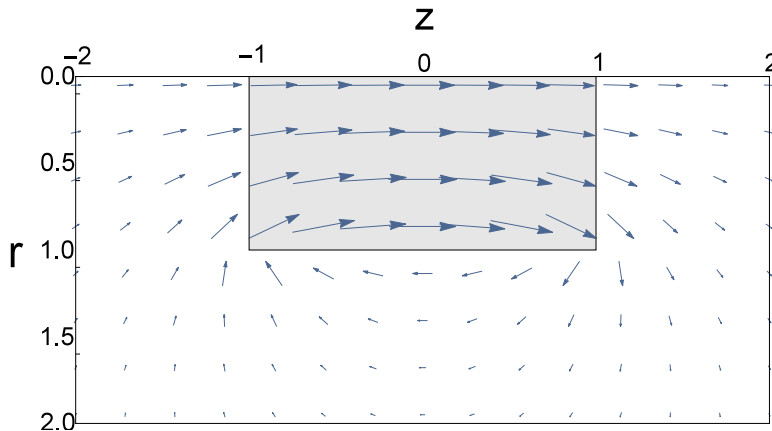


FIG. 2: Vector plot of the axisymmetric magnetic field $\mathbf{B}(r, z)$ generated by a finite continuous solenoid, Eqs. (1)-(3), for radius $a = 1$, length $L = 2$, and current density $\iota = 1$. Vectors are shown only for $r \geq 0$ so only the lower half of the solenoid (gray region) and half of the magnetic field are shown. The internal field is approximately uniform despite the solenoid's short length. Even for this short length, the interior magnetic field has attained a magnitude $B \approx 0.8B_0$ at the solenoid's center $r = z = 0$, where B_0 is defined in

Eq. (5).

Fig. 2 shows a vector-field plot of the magnetic field \mathbf{B} generated by Eqs. (2) and (3) for a solenoid of radius $a = 1$, length $L = 2$, and current density $\iota = 1$. Even for this short length, the interior magnetic field is approximately uniform and the magnetic field at the solenoid's center $r = z = 0$ has attained a magnitude $B \approx 0.8B_0$ that nearly equals the magnitude

$$B_0 = \mu_0 \iota, \quad (5)$$

of the uniform internal magnetic field of an infinitely long solenoid with the same current density ι . We note that Eq. (5) is the familiar formula¹ $B = \mu_0 n I$ for the magnetic field magnitude inside a long solenoid that is uniformly wound with n wires per unit length and with each wire carrying a current I . The product nI has units of current per length and corresponds to the current density ι in the limit $n \rightarrow \infty$, $I \rightarrow 0$ with nI finite.

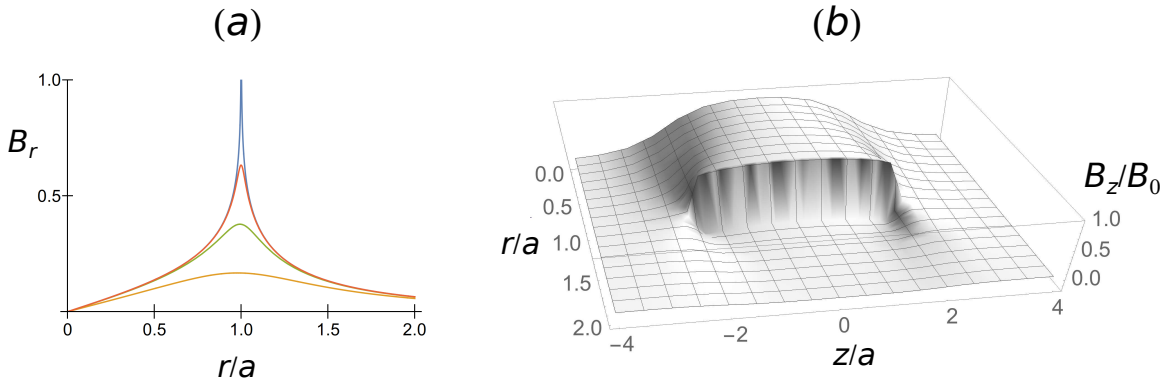


FIG. 3: The magnetic field $\mathbf{B}(r, z)$ of a finite continuous solenoid has two discontinuities, here shown for parameters $a = 1$, length $L = 4$, and unit current density $\iota = 1$. (a) The radial component $B_r(r, z)$ diverges for $z = \pm L/2$ at $r = a$. Here we show four curves of $B_z(r, z)$ for $z = 0.8(L/2), 0.95(L/2), 0.99(L/2)$, and $L/2$ (from lowest to highest curves). The curve for $z = L/2$ (and similar curve for $z = -L/2$) shows a divergence of B_r at $r = a$. One can show from Eq. (2) that this is a logarithmic divergence of the form $\ln(|r - a|)$ for r sufficiently close to a and for $z = \pm L/2$. (b) The axial component $B_z(r, z)$ has a jump discontinuity for $-L/2 \leq z \leq L/2$ at $r = a$ that represents the change in direction and magnitude of the magnetic field as one progresses radially from just inside to just outside the surface of the solenoid on a line of constant z .

It is difficult to see from Fig. 2 that the magnetic field of a finite continuous solenoid has two kinds of discontinuities. Fig. 3(a) shows how the radial component $B_r(r, z)$ varies with r

for fixed z , for several different values of z that approach a singularity at $r = a$ that occurs for $z = \pm L/2$. (So B_r diverges everywhere on the two ends of the solenoid at $z = \pm L/2$, which is again an artifact of our approximating the solenoid as a zero-thickness surface; this singularity does not occur for a solenoid of finite thickness with a corresponding volumetric current density J .) By setting $z = L/2$ in Eq. (2), one can evaluate the integral analytically over the range $0 \leq r \leq a - \epsilon$ and then find that the integral has a term proportional to $\ln(\epsilon)$ and so diverges logarithmically in the limit $\epsilon \rightarrow 0$. This will imply that the total energy associated with the magnetic field (Eq. (7) below) is a finite quantity.

The surface plot of the axial component $B_z(r, z)$ in Fig. 3(b) shows a more familiar discontinuity, that the z -component B_z of the magnetic field abruptly changes direction and magnitude as one passes radially from just inside to just outside the surface of the solenoid. (This is also apparent from Fig. 2 for r near $r = 1$ and $z = 0$, you can see how the magnetic field \mathbf{B} changes direction and magnitude near the surface of the solenoid.)

We next discuss how the external magnetic field of the finite continuous solenoid decreases with increasing length L for fixed radius a and for fixed current density ι , an important issue for our discussion in later sections regarding how large can the magnitude of the external magnetic field be for multiple parallel continuous solenoids of some given length L . Here there is some prior analytical insight via Exercise 5.61 on page 254 of Griffith's textbook on electrodynamics², which states that the magnetic field on the solenoid's midplane ($z = 0$) far from the axis ($r \gg a$) asymptotically has the form $\mathbf{B} = -B\hat{z}$, where the magnitude B is

$$B \approx \mu_0 \iota \times \frac{La^2}{4(r^2 + (L/2)^2)^{3/2}}. \quad (6)$$

This is the leading-order term in an expansion in powers of the small quantity a/r and so its validity when a/r is not small, say close to the surface of the solenoid, when $r \simeq a$, is not known.

Equation (6) makes two predictions. First, for sufficiently large solenoid lengths $L \gg r$, $B_z \propto L^{-2}$ so B_z decays rather slowly (algebraically rather than exponentially) to zero with increasing L . We note that this $1/L^2$ scaling is also how the magnetic field at the center of the solenoid, $r = z = 0$, converges to its infinite-length value Eq. (5) i.e. $(B_z - B_0)/B_0 \propto L^{-2}$ for sufficiently large L . (This follows from the analytical expression for the magnetic field on the axis of a finite solenoid, see Eq. (A8) in Appendix A.) Second, if this expression has validity for general values of r , Eq. (6) predicts that at a fixed radial distance r from the

axis, B does not decrease monotonically with increasing L , but first increases with a local maximum at $L_{\max} = \sqrt{2}r$, and then asymptotically decays to zero as $1/L^2$.

In Fig. 4, we compare these predictions with the exact analytical field of Eqs (2) and (3) for radial distances that are close to and far from the solenoid’s surface. Panel (a) shows that, for the representative fixed radial values $r = 1.1a$, $2a$ and $4a$ on the $z = 0$ symmetry plane, the z -component of the magnetic field $B_z(r, L)$ indeed first increases and then decreases with increasing L as suggested by Eq. (6), even for relatively short solenoids for which $L/a \gtrsim 2$. Surprisingly, the L -dependence of the analytical field at some fixed r is accurately described by Eq. (6) even for distances close to the solenoid ($r \gtrsim 2a$). Panel (b) shows a complementary result, that even for modest fixed solenoid lengths ($L \gtrsim 4a$), Eq. (6) also describes the radial dependence $B_z(r, 0)$ well, even for radii close to the outer surface of the solenoid. We conclude that Eq. (6) can be used as a quick and easy way to determine the magnitude of the magnetic field on the symmetry plane $z = 0$ of configurations of parallel solenoids without having to evaluate the integral Eq. (3).

The analytical result Eq. (A8) for B_z on the axis of a finite continuous solenoid shows that solenoids whose lengths $L \gtrsim 4a$ are already “sufficiently long” in the sense that the magnetic field magnitude $|B_z(r = 0, z = 0)|$ at the solenoid’s center already exceeds 90% of its infinite-length value $\mu_0\iota$. It occurred to the authors that an alternative way to identify when a solenoid is “sufficiently long” would be to ask for what length L^* (for a given radius a and given current density ι) does the energy U_{ext} associated with the magnetic field

$$U = \int \frac{B^2}{2\mu_0} d^3\mathbf{r} = \frac{1}{2\mu_0} \iint 2\pi r (B_r^2 + B_z^2) dr dz \quad (7)$$

external to the solenoid (the infinite region defined by $r > a$ or $|z| > L/2$), become less than half of the total energy U_{tot} associated with the entire magnetic field (Eq. (7) evaluated over all of space, $r \geq 0$). By approximating the integral Eq. (7) numerically (see Appendix A), we calculated and show in Fig. 5 the ratio $U_{\text{ext}}/U_{\text{tot}}$, as a function of solenoid length L for parameters $a = 1$ and $\iota = 1$. This ratio falls below the value $1/2$ for $L \approx 0.69a$ so that, even for quite short solenoids, the energy associated with the magnetic field inside the solenoid exceeds the energy associated with the external field, even though the latter has infinite spatial extent.

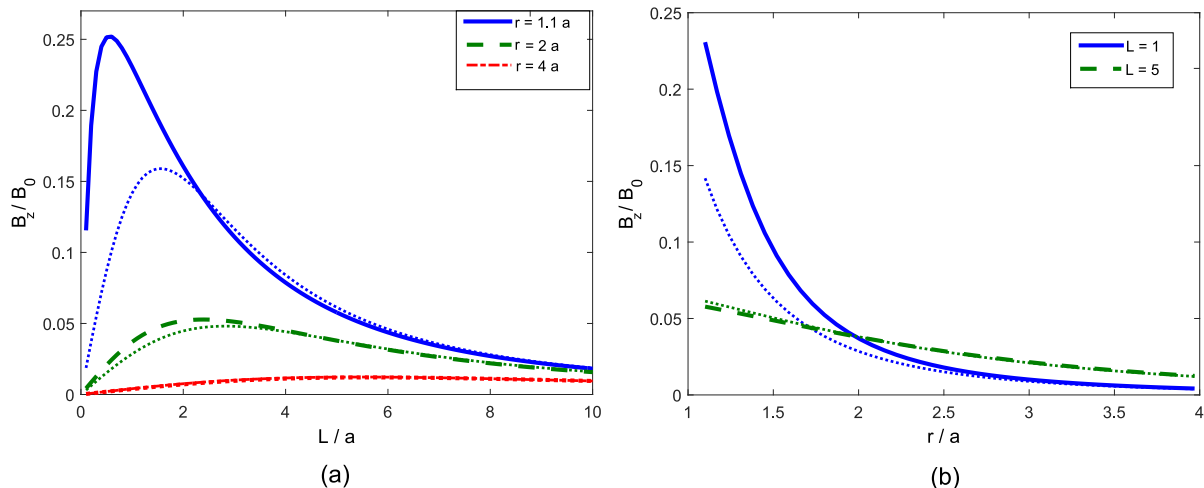


FIG. 4: (a) Comparison of Griffiths' result, Eq. (6), with the external magnetic field $B_z(r, z = 0)$ of a single finite continuous solenoid, normalized to the infinite solenoid axial value B_0 (Eq. (5)) versus the solenoid length L/a . Results are shown for three representative radial values, with the dotted lines showing Griffiths' corresponding result.

Note how B_z first increases and then decreases with increasing L . For $r = 4a$, the analytical result is the same as Eq. (6) to the accuracy of the plot. (b) The asymptotic result Eq. (6) for $B_z(r, 0)$ derived for $r \gg a$ (dotted lines) accurately describes the radial dependence of the analytical field $B_z(r)$ even for r close to the surface of the solenoid, provided that $L \gtrsim 4a$. The analytical result and numerical results are indistinguishable at the level of these plots for $L/a \geq 7$.

III. THE MAGNETIC FIELD OF A RING OF IDENTICAL PARALLEL FINITE CONTINUOUS SOLENOIDS

We are interested in the question of whether the magnetic field external to multiple parallel finite solenoids can ever be substantial in magnitude (comparable to the value $B_0 = \mu_0 \iota$ on the axis of an infinite solenoid) and approximately uniform. In this section, we consider an arrangement of $n \geq 3$ parallel identical finite continuous solenoids, each with current density $\iota = 1$ and of length L , that are arranged in a ring as shown in Figs. 6 and 1(a). Each solenoid is tangent to an inner common cylindrical surface of radius R and tangent to its neighbors. Because a substantial portion (nearly 50% in the case of many solenoids) of the external magnetic field of each solenoid passes through the common central

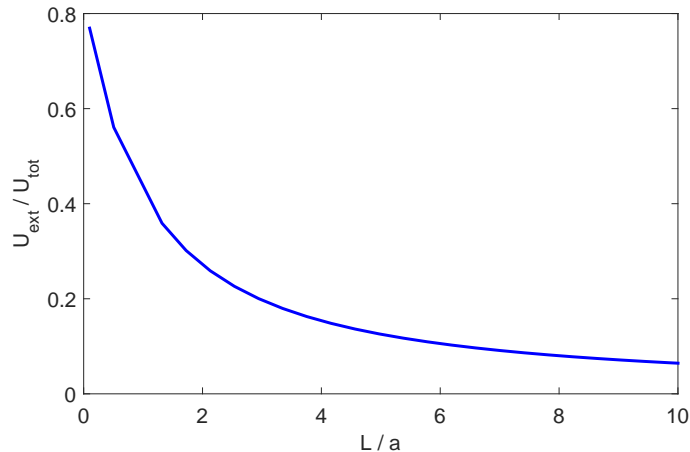


FIG. 5: Ratio of the energy U_{ext} , Eq. (7), associated with the magnetic field external to the solenoid ($r > a$ or $|z| > L/2$) to the total magnetic energy U_{tot} over all of space for a single continuous solenoid of fixed radius $a = 1$ and fixed current density ι , as a function of solenoid length L . The energy associated with the magnetic field inside the solenoid already exceeds the energy associated with the external magnetic field for short solenoids such that $L > 0.69a$.

cylindrical region, this ring geometry is a plausible candidate for producing an external magnetic field of substantial magnitude. We show in this section that this ring geometry can indeed produce a substantial magnetic field for solenoids that are long compared to their radii, but that the magnetic field in the common cylindrical region is generally not uniform. In the following section, Section IV, we discuss similar questions for a large finite hexagonal array of parallel finite continuous solenoids.

To describe the external magnetic field in the central cylindrical region, we introduce a second cylindrical coordinate system (ρ, ϕ, z) such that $\rho = 0$ corresponds to the axis of the inner cylindrical surface, $\rho = R$ corresponds to the cylindrical surface that all the solenoids are tangent to, and $z = 0$ is the common bisecting plane of the parallel solenoids. For n parallel solenoids that are all tangent to the inner cylindrical surface of radius R and tangent to neighbors, the tangency conditions imply that the common solenoid radius a_n is given by

$$a_n = \frac{\sin(\pi/n)}{1 - \sin(\pi/n)} R, \quad n \geq 3, \quad (8)$$

so $a_3 \approx 6.5R$, $a_4 \approx 2.4R$, $a_5 \approx 1.4R$, $a_6 = R$, and $a \approx \pi R/n$ becomes small for large n .

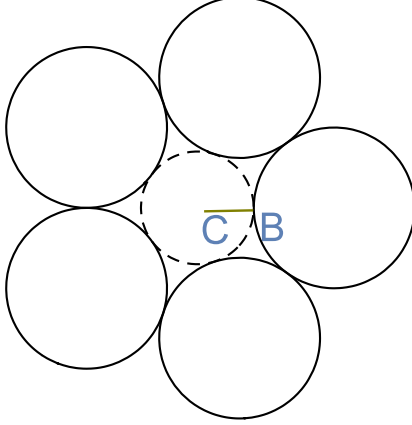
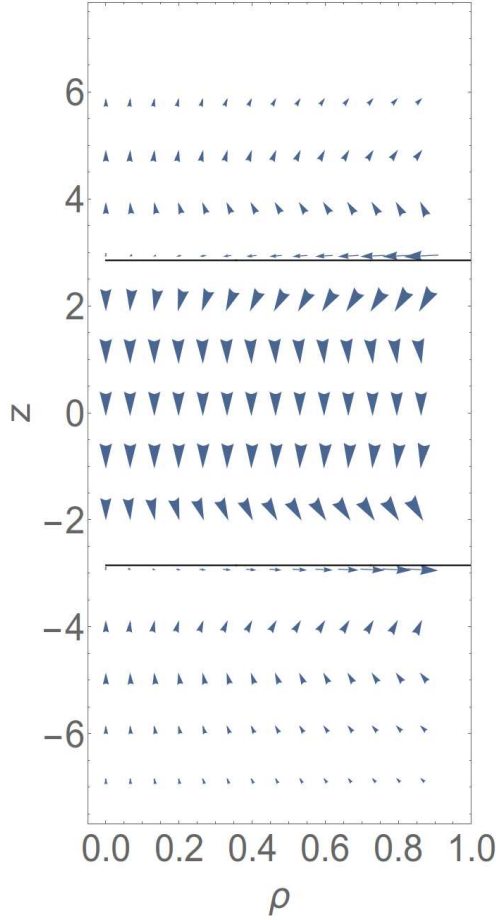


FIG. 6: Cross-section of a ring of $n = 5$ parallel continuous solenoids of length $L = 2$ and radius $r \approx 1.4$ that are tangent to neighboring solenoids and to a common inner cylindrical surface of radius $R = 1$, shown as a dotted ring with center C . The line segment CB denotes the location of the rectangular area, transverse to the plane of the figure, in which the magnetic field \mathbf{B} is plotted in Fig. 7. For a perspective drawing, see Fig. 1(a).

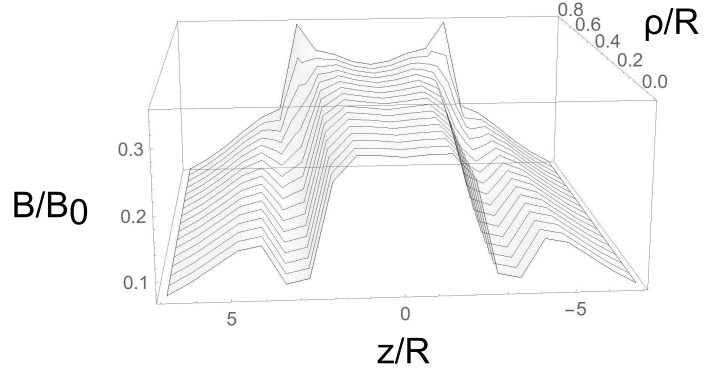
At any point (ρ, ϕ, z) inside the central cylindrical region $\rho \leq R$, the z -component of the magnetic field $B_z(\rho, \phi, z)$ is obtained by directly adding the values $B_z(r_i, z)$ from each solenoid in the ring at that point, where r_i is the distance of the point (ρ, ϕ, z) to the axis of the i th solenoid. Calculating the radial component $B_\rho(\rho, \phi, z)$ is more involved since the radial direction $\hat{\mathbf{r}}_i$ with respect to the i th solenoid at (ρ, ϕ, z) varies with i . The details are given in Appendix B.

We now discuss our calculations of the magnetic field in the central cylindrical region for rings with varying number n of continuous solenoids and varying length L , for a central cylindrical region of fixed radius $R = 1$ and for all solenoids having the same current density $\iota = 1$.

For a ring of $n = 5$ solenoids of radius $a \approx 1.4$ (see Eq. (8)) and length $L = 4a$, Fig. 7(a) shows a vector plot of the magnetic field $\mathbf{B}(\rho, \phi, z)$ inside the central cylindrical region $0 \leq \rho \leq R$ along the plane $\phi = 0$, which corresponds to a rectangle that is perpendicular to and passes through the line segment CB in Fig 6(b). We see that the magnetic field is approximately uniform in direction and magnitude with a magnitude $B/B_0 \approx 0.3$ that is about one third the magnitude of the magnetic field $B_0 = \mu_0\iota$ found on the axis of an infinitely long single solenoid with the same current density ι . The magnetic field deviates substantially from that of a single solenoid (see Fig. 2) in the planes $z = \pm L/2 \approx \pm 2.8$,



(a)



(b)

FIG. 7: External magnetic field produced by 5 parallel continuous solenoids tangent to an inner cylinder of radius $R = 1$, for solenoid length $L = 4a \approx 5.6$ where the solenoid radius $a \approx 1.4$. (a) Vector plot of $\mathbf{B}(\rho, z)$ in the plane $\phi = 0$ (line CB of Fig. 6(b)) shows the direction and magnitude of the magnetic field inside the central cylindrical region. The lengths of the vector heads are proportional to the local magnitude B . (b) Surface plot of field magnitude B/B_0 normalized to the magnetic field magnitude B_0 inside an infinite single solenoid of the same current density ι .

which are indicated by the horizontal black lines in Fig. 7(a); the magnetic field is purely horizontal and of greatly decreased magnitude.

Further insight about the structure of the central magnetic field is provided by panel (b) of Fig. 7, which shows a surface plot of the field magnitude $B(\rho, z)$ for the same rectangle as panel (a). Panel (b) confirms that the magnetic field is approximately uniform inside the

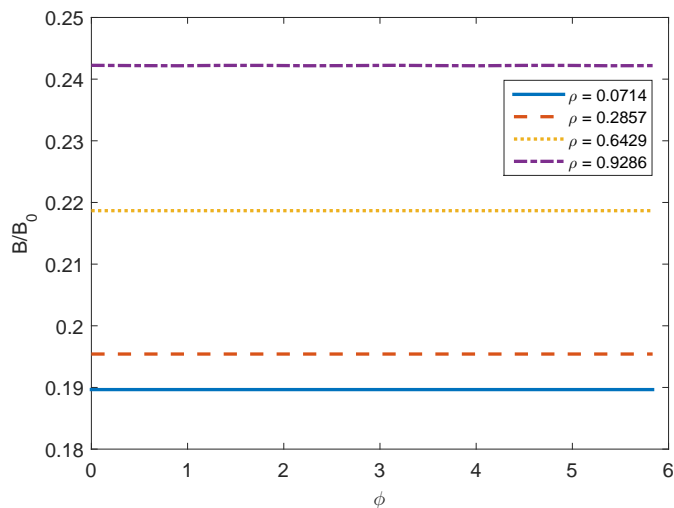


FIG. 8: Plot of $B_z(\rho, \phi, z = 0)$ inside the inner cylindrical surface of an arrangement of five solenoids each with $L/a = 4$ and $\iota = 1$, for $\rho = 0.07, 0.29, 0.64$ and 0.93 . The magnetic field has high azimuthal symmetry, despite there being five discrete sources of magnetic field.

There is only evidence of a five-fold symmetry close to the edges of the solenoids.

central cylindrical region (the magnitude B is approximately constant for $|z| \leq L/2$) but becomes non-uniform near the boundary of one of the solenoids because of the divergence of B_r near the ends of the solenoid (see Fig. 3(a)).

Fig. 8 shows that the magnetic field inside the cylindrical region is highly axisymmetric for $z = 0$. Despite the fact that the field is being generated by five discrete solenoids, there is graphical evidence of a five-fold symmetry only for r close to R and for $z \simeq \pm L/2$, as shown in Fig 7(b).

We found that the external magnetic field in the central cylindrical region becomes more nonuniform and decays radially in magnitude for larger numbers of solenoids ($n > 4$) so Fig. 7 is close to the best case in terms of achieving a uniform magnetic field in a ring geometry. As the number n of solenoids increases for fixed R and fixed L , the solenoid radii a_n Eq. (8) decrease in size, the solenoids effectively become longer compared to their radius, and so the magnetic field external to each solenoid decreases in magnitude according to Eq. (6), being largest near the surfaces of the solenoids ($\rho \approx 1$) and decreasing towards the center of the common cylindrical region where $\rho = 0$. This is illustrated in Fig. 9 which shows how $B_z/B_0(\rho, \phi = 0, z = 0)$ varies on the bisecting plane $z = 0$ for increasing values

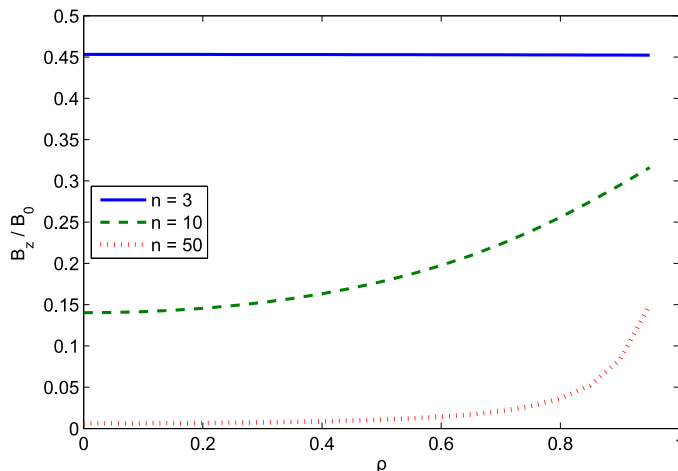


FIG. 9: Axial component $B_z(\rho, z = 0)$ on the bisection plane $z = 0$ for $n = 3, 10,$ and 50 solenoids, for fixed solenoid length $L/a = 4$ and fixed current density ι . The increase in the number n of sources cannot compensate for the $1/L^2$ decrease in magnetic field strength so the magnetic field in the central cylindrical region becomes small for large n .

of solenoid number n , for a fixed length $L/a = 4$.

IV. THE MAGNETIC FIELD OF AN HEXAGONAL ARRAY OF IDENTICAL PARALLEL CONTINUOUS SOLENOIDS

The second configuration of parallel finite solenoids that we explore is a large finite hexagonal lattice. Since we have shown in Fig 4 of Sec. II that the external magnetic field of a single solenoid can be as large as $0.25B_0$ on axis, just outside the solenoid, this geometry is a potential candidate for producing an external magnetic field of substantial magnitude (at least for specific solenoid lengths and spacings).

We define an hexagonal Bravais lattice¹² such that the locations \mathbf{v} of each solenoid axis in the $z = 0$ plane are given by the two-dimensional vectors

$$\mathbf{v} = s(m\mathbf{v}_1 + n\mathbf{v}_2) + \mathbf{v}_3, \quad (9)$$

where the coefficients m and n go over all possible integers, and where the positive parameter s denotes the lattice spacing (distance between two nearest neighbor solenoid axes). The

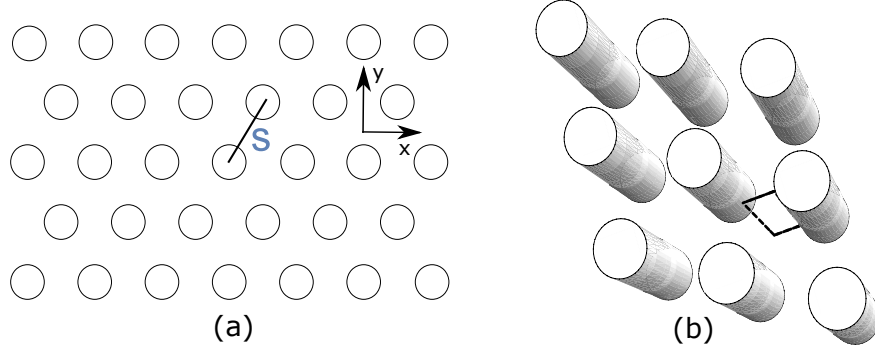


FIG. 10: (a) Horizontal cross-section through a portion of an hexagonal lattice of parallel continuous solenoids for lattice spacing $s = 1$ as defined by Eq 9 and 10. The common radius of the solenoids was chosen to be $a = 1/4$. Also shown are the directions of the coordinates x and y .(b) Perspective drawing of a section of the lattice. The black dashed rectangle corresponds to the region in which we compute the magnetic field shown in Figure 12.

basis vectors \mathbf{v}_1 and \mathbf{v}_2 are given by

$$\mathbf{v}_1 = \hat{\mathbf{i}}, \quad \text{and} \quad \mathbf{v}_2 = \left(\frac{-1}{2}\right)\hat{\mathbf{i}} + \frac{\sqrt{3}}{2}\hat{\mathbf{j}}. \quad (10)$$

The vector \mathbf{v}_3 , which here is $(1/2)\hat{\mathbf{i}} + (1/2\sqrt{3})\hat{\mathbf{j}}$, shifts the lattice relative to the origin of the coordinate system and places the origin at the centroid of the triangle formed by three nearest-neighbour solenoids. For a given lattice spacing s , the solenoid radius a must satisfy $a < s/2$ so that that the solenoid surfaces do not intersect.

The array of solenoids is characterized by the lattice spacing s and the length-to-radius ratio L/a of each of the solenoids. We introduce an xyz -Cartesian coordinate system, where the origin $(x, y, z) = (0, 0, 0)$ corresponds to the centroid of the triangle formed by the centers of three nearest-neighbour solenoids in a cell of the hexagonal lattice. Again, $z = 0$ corresponds to the bisecting plane of the solenoids.

We approximate the total magnetic field near the origin for an infinite period lattice was found by summing the fields from many solenoids in a large, finite, approximately circular region centered on $(0, 0, 0)$. Fig. 11 shows the component B_z at $(0, 0, 0)$ as a function of the radius of the area from which fields of individual solenoids were summed. Summing the fields from an area of the hexagonal array with radius $100s$ is sufficient to approximate the magnetic field due to the infinite array with a relative accuracy better than 0.05.

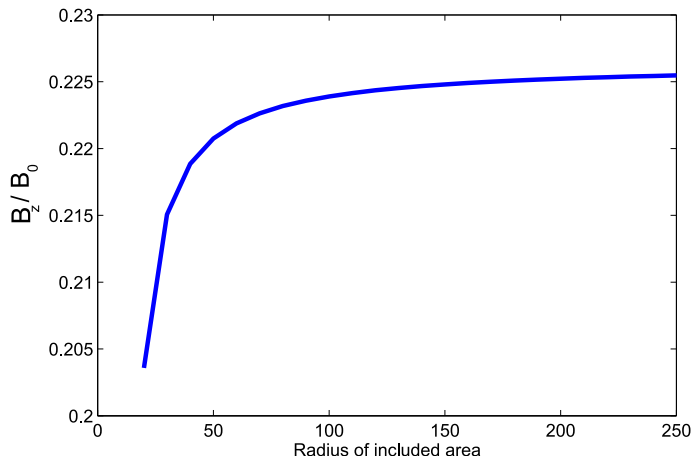


FIG. 11: Plot of the magnetic field component B_z/B_0 at the centroid of three solenoids in an hexagonal lattice as a function of the radius R of a circle centered at the centroid. For the largest radius $R/s = 500$ (not shown), there are $\sim 750,000$ solenoids enclosed within the circle. Note how over the range $30 < R < 500$, B_z varies only by about 10%, and furthermore appears to asymptote to a finite value. A circle of radius $= 100s$ already approximates the infinite lattice case to better than 5%.

The magnetic field at a given point (x, y, z) was computed by individually summing the components of the magnetic field from the solenoids in the lattice from a region with radius $100s$ (see Appendix B). The field within each unit cell of the hexagonal lattice is again axisymmetric. Further details of the structure of the magnetic field within a single cell of the lattice are shown in Fig. 12, which is a vector field plot of the magnetic field in the plane defined by the line section marked BC in Fig. 10 and with axial coordinates between $z = \pm L$. The external magnetic field away from the edges of the solenoid is comparable in uniformity to the magnetic field inside the solenoid, with a magnitude $B_z = 0.6B_0$. This external magnetic field is quite uniform for most of $z \leq |L/2|$, unlike the central magnetic field described in Sec. III.

We also found that the magnetic field $B_z(0, 0, 0)$ decreases approximately algebraically as a function of the lattice size s for fixed a and L . Fig 13 shows how the magnetic field $B_z(0, 0, 0)$ decreases in magnitude with increasing lattice size s for parameter values $\iota = 1$, $a = 1/4$, and $L = 0.1, 5, 50$, and 100 . The decay of B_z to 0 follows an approximate power law with a numerical exponent that approaches -2 with increasing solenoid length.

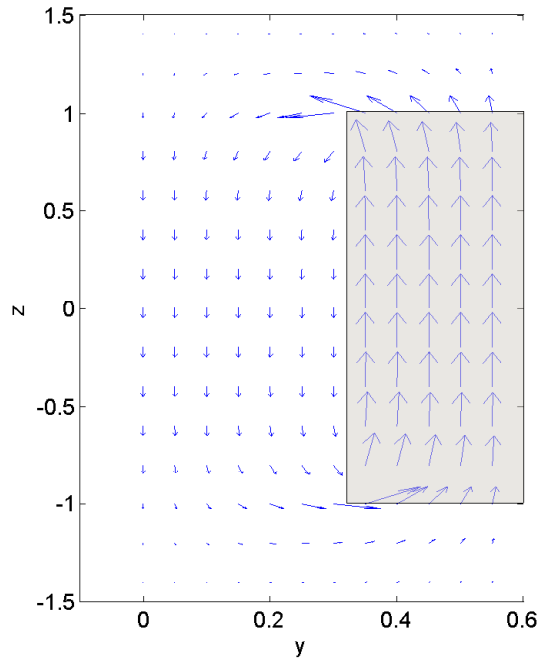


FIG. 12: Plot of the magnetic vector field \mathbf{B} generated between solenoids in a hexagonal lattice in the black dashed rectangle shown in Fig. 10(b), with $s = 1$, $a = 1/4$, $\iota = 1$, and $L/a = 8$, summed over solenoids in a circular area with radius $R = 100$. The location of the solenoid is indicated by a gray rectangle. Only the in-plane components of the magnetic field are non-zero. The magnetic field is highly uniform in the region external to solenoids, for $|z| < L/2$.

Furthermore, we find that the magnitude of the magnetic field for any given lattice spacing depends nonmonotonically on the length of the solenoid. However, this dependence is small: for fixed s , we observe in Fig. 13 that changing the lattice spacing by a factor of 20 decreases B_z/B_0 only by a factor of ≈ 0.5 .

This slow decay of B_z/B_0 towards zero as a function of L , for fixed s , can be seen more clearly in Fig. 14, which shows $B_z(0, 0, 0)/B_0$ as a function of L/a for $a = 1/4$, $s = 1$, and $\iota = 1$. As expected from our discussion of the external magnetic field of the single solenoid, the decay of B_z is nonmonotonic. However, after reaching a local maximum, B_z decays linearly, with a numerically derived functional form $B_z = -0.0045L + 0.63$, from which we extrapolate that B_z decays to 0 only for a solenoid length of ~ 140 . This linear decay of the external magnetic field of the single solenoid provides another example of a feature of the

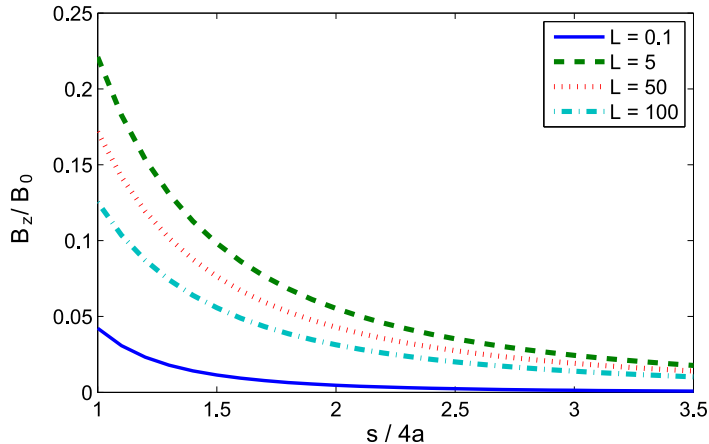


FIG. 13: Plot of the ratio $B_z(0, 0, 0)/B_0$ as a function of the lattice spacing s for an hexagonal array of parallel identical solenoids of length $L = 0.1, 5, 50$ and 100 , radius $a = 1/4$, and current density $\iota = 1$. The decay of B_z towards 0 follows a power law with a numerically derived exponent that approaches -2 for increasing L , consistent with Eq. (6).

magnetic field that would have been difficult to predict without carrying out a numerical study.

V. CONCLUSIONS

In this paper, we have investigated using elementary methods that sophomore physics and engineering students can understand (numerical approximations to one-dimensional integrals and superposition by direct summation) whether the magnetic field external to some arrangement of identical parallel finite solenoids of radius a , length L , and uniform current density ι can ever be substantial in magnitude and possibly uniform. Our motivation was to provide a deeper insight to the properties of the magnetic field external to a finite solenoid, which in many undergraduate physics textbook is ignored because its magnitude is known to become negligibly small for solenoids that are sufficiently long compared to their radii (although what is meant by “sufficiently long” is rarely discussed).

We were also interested in the question of whether the supposedly small external magnetic field could ever be made substantial (compared to the magnetic field magnitude Eq. (5) inside an infinitely long solenoid of identical current density) and possibly highly uniform

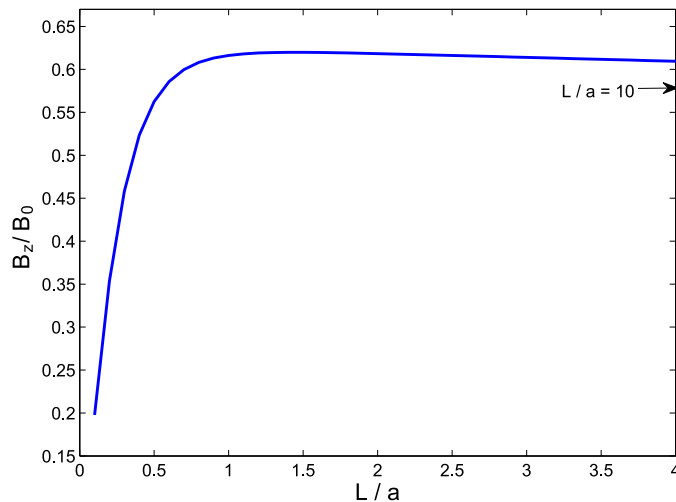


FIG. 14: Plot of the ratio $B_z(0, 0, 0)/B_0$ as a function of the solenoid length L for an hexagonal array of solenoids. For $L/a = 10$, B_z/B_0 reaches a value of 0.58, as marked by an arrow. The magnetic field attains a local maximum at $L = 2$ of about half the field of a single finite solenoid, after which it decays slowly towards the infinite length limit of $B_z = 0$.

by combining the magnetic fields of many parallel identical finite solenoids. This question is not easy to answer, say by applying Ampère’s law to some small rectangular loop as is commonly done in undergraduate physics textbooks to a single infinite solenoid^{1,2}, since one does not know in advance the symmetry of the magnetic field, e.g., whether it is everywhere parallel to the axes of the solenoids, and uniform in magnitude.

We studied two configurations of identical parallel solenoids with high symmetry since high symmetry should favor uniformity of the external field. One configuration consisted of a ring of n parallel solenoids that each are tangent to nearest neighbors and to a common inner cylindrical surface (see Fig. 6). The second configuration was a large, finite, roughly circular hexagonal array of parallel solenoids (see Fig. 10), that we used to approximate the magnetic field generated by an infinite hexagonal array of parallel solenoids. For both cases, we investigated how the external magnetic field depended on the radius, length, and spacing of the solenoids, while the current density was kept fixed.

For the ring geometry and hexagonal array, we found that the external magnetic field could have a substantial magnitude, even for solenoids that are long compared to their radii.

But only for the magnetic field generated by a large hexagonal array did we find that the external magnetic field could also be highly uniform, at least in regions of space that lies between the two planes that contain the ends of the solenoids.

The starting point for our analysis was an exact analytical expression, Eqs. (1)-Eq. (3), in terms of two one-dimensional integrals for the axisymmetric magnetic field \mathbf{B} produced by a single finite continuous solenoid. It turns out that these one-dimensional integrals can be rapidly and accurately approximated at all points in space (except for points near the edges $r = a$ and $z = \pm L/2$ of the solenoid, where the radial component B_r diverges logarithmically) to better than eight significant digits using simple and straightforward invocations of functions provided by the mathematics program Mathematica⁸ (see Fig. 15 as an example). The same Mathematica program provided easily used tools to add up the magnetic fields of many solenoids by superposition, and then visualize the resulting magnetic field.

Thus this paper, in addition to providing new insights about the magnetic field generated by a single solenoid and by groups of solenoids, should provide a useful example to share with undergraduate physics students about how mathematics software environments like Mathematica can be used to explore physics problems that are substantially more challenging and more interesting than what can be analyzed by analytical methods. Based on our experience, we feel that such software should be more widely and systematically incorporated into undergraduate physics courses so that students learn how to use analytical, numerical, and visual ways to understand or explore a variety of physics problems.

Appendix A: Validation of the numerical calculations

The Mathematica code needed to carry out the calculations discussed in previous sections is modest, about four pages in length. But it took some effort to determine whether the results were correct and their accuracy. We summarize in this section some of the steps we took to validate the results.

We used the Mathematica function `NIntegrate` to approximate the key one-dimensional integrals, Eqs. (2) and (3), that give the cylindrical components B_r and B_z of the magnetic field generated by a finite solenoid. Details about this function are available through the freely accessible URL reference.wolfram.com/language/ref/NIntegrate.html, so we mention briefly that this function takes as its arguments some integrand in symbolic

form and the bounds of the definite integral (see Fig. 15) plus many possible optional parameters. (We used the default parameters and obtained acceptable accuracy as mentioned further below.) This function then uses an unspecified adaptive integration algorithm to numerically approximate the definite integral to some specified accuracy.

```

bzSolenoid[ r_, z_, a_, L_ ] := Module[
  {ξp, ξn, ι = 1., μ0 = 4. * π * 10-7},
  ξp = z + L/2;
  ξn = z - L/2;
   $\frac{a \mu_0 \iota}{2 \pi}$  * NIntegrate[
     $\frac{(a - r \text{Cos}[\alpha])}{(r^2 + a^2 - 2 a r \text{Cos}[\alpha])}$   $\left( \frac{\xi_p}{(\xi_p^2 + r^2 + a^2 - 2 a r \text{Cos}[\alpha])^{0.5}} - \frac{\xi_n}{(\xi_n^2 + r^2 + a^2 - 2 a r \text{Cos}[\alpha])^{0.5}} \right)$ 
    , {α, 0, π}
  ]
];

```

FIG. 15: Mathematica code that uses the Mathematica adaptive numerical integration function NIntegrate to approximate the magnetic field component $B_z(r, z, a, L)$ given by Eq. (3) at a point (r, z) in space, for a solenoid of radius a , length L , and current density $\iota = 1$.

We tested the accuracy of the numerical values returned by NIntegrate for Eqs. (2) and (3) by comparing their values with analytically equivalent expressions that use entirely different numerical algorithms for their approximation. Researchers have shown^{11,13}, that Eqs. (2) and (3) can be expressed in terms of elliptic integrals¹⁴ as follows

$$B_r = \frac{\mu_0 \iota}{\pi} \sqrt{\frac{a}{r}} \left[\frac{E(k^2)}{k} + \frac{k^2 - 2}{2k} K(k^2) \right]_{\xi_-}^{\xi_+} v, \quad (\text{A1})$$

$$B_z = \frac{\mu_0 \iota}{4\pi} \frac{1}{\sqrt{ar}} \left[\xi k \left(K(k^2) + \frac{a - r}{a + r} \Pi(h^2, k^2) \right) \right]_{\xi_-}^{\xi_+}, \quad (\text{A2})$$

where the symbols and functions have the following definitions:

$$k^2 = \frac{4ar}{\xi^2 + (a+r)^2}, \quad (\text{A3})$$

$$h^2 = \frac{4ar}{(a+r)^2 + \xi^2}, \quad (\text{A4})$$

$$K(m) = \int_0^{\pi/2} \frac{d\theta}{\sqrt{1 - m \sin^2 \theta}}, \quad (\text{A5})$$

$$E(m) = \int_0^{\pi/2} \sqrt{1 - m \sin^2 \theta} d\theta, \quad (\text{A6})$$

$$\Pi(n, m) = \int_0^{\pi/2} \frac{d\theta}{(1 - n \sin^2 \theta) \sqrt{1 - m \sin^2 \theta}}. \quad (\text{A7})$$

The algorithms used by Mathematica to approximate elliptic integrals numerically use a completely different method than the adaptive integration algorithm of the `NIntegrate` function. Our comparison of Eqs. (2) and (3) with Eqs. (A1) and (A2) showed that both expressions gave relative errors of better than 10^{-8} (eight significant digits) for points near and far from the solenoid's surface. This accuracy was sufficient for the goals of this paper.

Some further tests we made to validate our results were the following:

1. We verified that Eq. (3) agrees accurately with the analytical expression for the magnetic field on the axis of a continuous solenoid with end surfaces at $z = \pm L/2$:

$$B_z(r=0, z) = \mu_0 \iota \times \frac{1}{2} \left(\frac{z + L/2}{\sqrt{(z + L/2)^2 + a^2}} - \frac{z - L/2}{\sqrt{(z - L/2)^2 + a^2}} \right). \quad (\text{A8})$$

This expression includes the limiting case $L \rightarrow 0$ when the solenoid reduces to a current loop of radius a and again the numerical approximations to the continuous solenoid were found to be accurate in that limit.

For $z = 0$, Eq. (A8) predicts that $B_z \approx \mu_0 \iota (1 - 2(a/L)^2 + \dots)$ to lowest order in $(a/L)^2$, i.e., the relative error $(B_z(0, 0) - \mu_0 \iota) / (\mu_0 \iota)$ decays as $1/L^2$ for large L . This $1/L^2$ convergence is similar to what is found for the solenoid's external field.

2. We verified that Eqs. (2) and (3)) converge to the corresponding components

$$B_r(r, z) = \frac{\mu_0 m}{4\pi} \frac{3rz}{(r^2 + z^2)^{5/2}}, \quad B_z(r, z) = \frac{\mu_0 m}{4\pi} \frac{2z^2 - r^2}{(r^2 + z^2)^{5/2}} \quad (\text{A9})$$

of the magnetic field of the continuous solenoid's equivalent point magnetic dipole at its center $r = z = 0$, with magnetic moment

$$m = (\pi a^2) \iota L, \quad (\text{A10})$$

when the distance $d = \sqrt{r^2 + z^2}$ of the point (r, z) of evaluation was large, $d \gg a, L$, compared to the solenoid's radius or length. That is, the solenoid's external magnetic field correctly converges to that of a point magnetic dipole far from the solenoid, with a $1/d^3$ decay in magnitude. Eq. (A10) was deduced by comparing Eq. (6) with the magnetic field of a point dipole $\mu_0 m / (4\pi r^3)$ for $z = 0$ in the far-field regime $r \gg L, a$.

3. We verified that the total magnetic field \mathbf{B} at points of certain symmetry had zero components, even though the numbers added to obtain the component were nonzero.

We also verified the convergence and accuracy of the 2D integral of magnetic energy, which presents two types of discontinuities, as shown in Fig. 16. Firstly, the peak at $r/a = 1$ and $z = L/2$ comes from a divergence of the radial component $B_r(r, z)$ of the magnetic field. Near the point of divergence, $B_r(r, \pm L/2) \approx \ln|r - a|$, which does lead to a convergent value for the external magnetic energy. Since the divergence due to the zero-thickness of the continuous solenoid leads to a finite magnetic energy, the magnetic energy of a physical solenoid wound with wires of finite thickness will show results compatible to those presented here.

Appendix B: Adding up radial components B_r from different solenoids

For both the ring geometry and hexagonal array, one has to add magnetic fields from different directions. We show the main issues for the ring geometry. The calculation of the total magnetic field $\mathbf{B}(\rho, \theta, z)$ at some point $P = (\rho, \theta, z)$ inside the common cylindrical surface $\rho = R$ of the ring of n solenoids described in Section III provides a nice example of how to change information described in the cylindrical coordinate system (r, ϕ, z) of one system (a given solenoid) to information described by the cylindrical coordinate system (ρ, θ, z) associated with the common cylindrical surface. The key issue is that the radial unit vector $\hat{\mathbf{r}}_i$ associated with the i th solenoid varies with i as shown in Fig. 18, so one has to accumulate the components of the vector $B_{r,i}\hat{\mathbf{r}}_i$ along the unit vectors $\hat{\boldsymbol{\rho}}$ and $\hat{\boldsymbol{\theta}}$ of the (ρ, θ, z) coordinate system. The z -component B_z is easier to compute since the z axes of the solenoids are all parallel to the z axis of the cylindrical surface.

If the radius a_n of each solenoid is given by Eq. 8, the axis of each solenoid lies on the

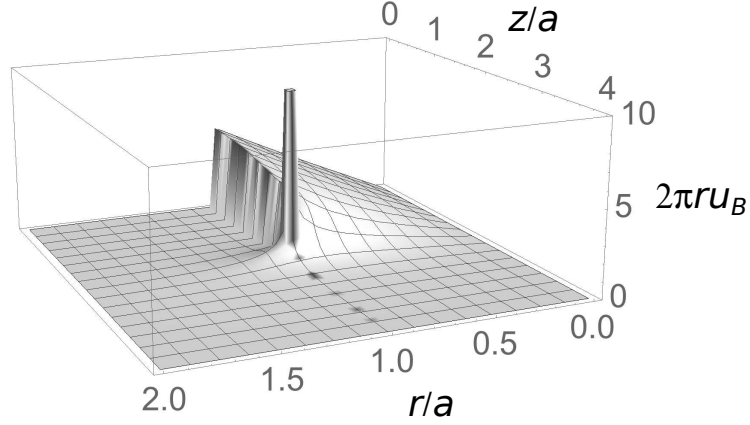


FIG. 16: Surface plot of the integrand $(2\pi r)[B^2/(2\mu_0)]$ of the magnetic energy, from Eq. (7) for the parameters $a = 1$, $L = 4$, and $\iota = 1$. The peak at $r/a = 1$ and $z = L/2$ comes from an integrable divergence of the radial component $B_r(r, z)$ of magnetic field (see Fig. 3(a)), while the line of discontinuity from $z = 0$ to $z = L/2$ along the line $r = a$ comes from the z -component B_z , which changes sign discontinuously as one passes from the inside to the outside of the solenoid (see Fig. 3(b)). The two discontinuities in the energy integrand lead to a challenging integral to approximate numerically.

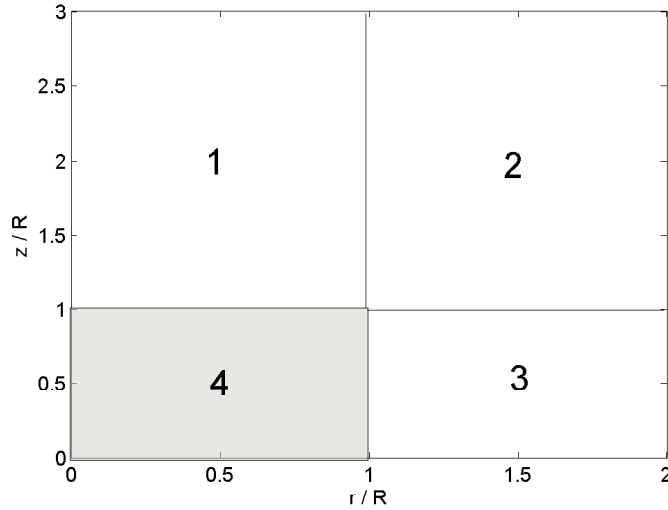


FIG. 17: Subdivided region of integration for calculation of external and internal energy. We use the symmetry of the solenoid to calculate the magnetic field only for the right side of the solenoid, $z \geq 0$.

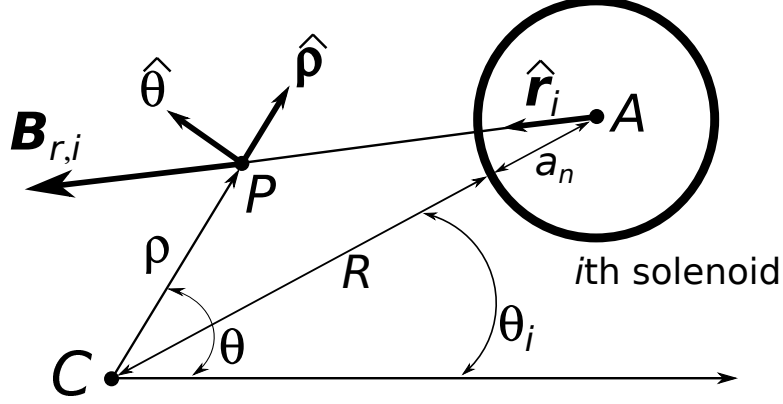


FIG. 18: Illustration showing how the total magnetic field \mathbf{B}_{tot} at a point $P = (\rho, \theta, z)$ inside the common cylindrical surface $\rho = R$ with axis at point C is obtained by adding the vectors $\mathbf{B}_{r,i} = B_{r,i}(r_i, z)\hat{\mathbf{r}}_i$ of the magnetic field created by the i th solenoid whose axis at point A has the coordinates $(\rho, \theta) = (R + a_n, \theta_i)$. The length r_i is the radial coordinate of the point P with respect to the solenoid's axis at A .

circle $\rho = R + a_n$ and has angular coordinate

$$\theta_i = \frac{2\pi}{n}(i - 1), \quad i = 1, \dots, n. \quad (\text{B1})$$

If we define the two-dimensional vectors

$$\hat{\boldsymbol{\rho}} = (\cos(\theta), \sin(\theta)), \quad (\text{B2})$$

$$\hat{\boldsymbol{\theta}} = (-\sin(\theta), \cos(\theta)), \quad (\text{B3})$$

$$\boldsymbol{\rho} = \rho \hat{\boldsymbol{\rho}}, \quad (\text{B4})$$

$$\mathbf{a}_i = (R + a_n) (\cos(\theta_i), \sin(\theta_i)), \quad (\text{B5})$$

then the vector $\boldsymbol{\rho} - \mathbf{a}_i$ points from the axis A of the i th solenoid to the point P , its Euclidean length r_i

$$r_i = \|\boldsymbol{\rho} - \mathbf{a}_i\|, \quad (\text{B6})$$

is the distance of the point P to the axis of the i th solenoid, and so the radial unit vector $\hat{\mathbf{r}}_i$ along the radial coordinate centered on the i th solenoid is given by

$$\hat{\mathbf{r}}_i = \frac{\boldsymbol{\rho} - \mathbf{a}_i}{r_i}. \quad (\text{B7})$$

With this notation, the radial and azimuthal components of the total magnetic field at the

point P are given by

$$B_\rho = \hat{\boldsymbol{\rho}} \cdot \sum_{i=1}^n B_{r,i} \hat{\mathbf{r}}_i, \quad (\text{B8})$$

$$B_\theta = \hat{\boldsymbol{\theta}} \cdot \sum_{i=1}^n B_{r,i} \hat{\mathbf{r}}_i, \quad (\text{B9})$$

where $B_{r,i} = B_r(r_i, z)$ is the radial component of the magnetic field Eq. (2) at a point a distance $r = r_i$ from the axis of the i th solenoid.

ACKNOWLEDGMENTS

We thank Stephen Teithsworth for helpful discussions.

* mxl2@duke.edu; Corresponding author

† hsg@phy.duke.edu

¹ H. Young and R. Freedman. *University Physics with Modern Physics*. Addison-Wesley, San Francisco, California, 13th edition, 2011.

² D. Griffiths. *Introduction to Electrodynamics*. Addison-Wesley, New Jersey, USA, 3rd edition, 1999.

³ E. Purcell and S. Morin. *Electricity and Magnetism*. Cambridge U. Press, New York, 3rd edition, 2013.

⁴ G. V. Brown and L. Flax. Superposition of semi-infinite solenoids for calculating magnetic fields of thick solenoids. *American Journal of Physics*, 1964.

⁵ J. Farley and R. H. Price. Field just outside a long solenoid. *American Journal of Physics*, 2001.

⁶ V. S. Bagnato S. R. Muniz and M. Bhattacharya. Analysis of off-axis solenoid fields using the magnetic scalar potential: An application to a zeeman-slower for cold atoms. *American Journal of Physics*, 2015.

⁷ N. Derby and S. Olbert. Cylindrical magnets and ideal solenoids. *American Journal of Physics*, 2009.

⁸ Wolfram Research, Inc. Mathematica, version 10.1. Champaign, Illinois, 2015.

- ⁹ Maplesoft. Maple, version 162, 2015.
- ¹⁰ MATLAB. *version 8.5.0.197613 (R2015a)*. The MathWorks Inc., Natick, Massachusetts, 2015.
- ¹¹ E. Callaghan and S. Maslen. The magnetic field of a finite solenoid. NASA Technical Note D-465, 1960.
- ¹² Neil W. Ashcroft and N. David Mermin. *Solid State Physics*. Holt, Rinehart and Winston, New York, 1976.
- ¹³ Solenoids. <http://en.wikipedia.org/wiki/Solenoid>. Accessed August 2014.
- ¹⁴ P. Morse and H. Feschbach. *Methods of Theoretical Physics*, volume 2. Feschbach Publishing, Minneapolis, MN, 2005.